

Electrical detection of spin accumulation and spin precession at room temperature in metallic spin valves

F.J. Jedema, M.V. Costache, H.B. Heersche, J.J.A. Baselmans, B.J. van Wees
*Department of Applied Physics and Materials Science Center, University of Groningen,
 Nijenborgh 4, 9747 AG Groningen, The Netherlands*
 (November 12, 2018)

We have fabricated a multi terminal lateral mesoscopic metallic spin valve demonstrating spin precession at room temperature, using tunnel barriers in combination with metallic ferromagnetic electrodes as spin injector and detector. The observed modulation of the output signal due to the spin precession is discussed and explained in terms of a time of flight experiment of electrons in a diffusive conductor. The obtained spin relaxation length $\lambda_{sf} = 500$ nm in an Al strip will make possible detailed studies of spin dependent transport phenomena and allow to explore the possibilities of the electron spin for new electronic applications at RT.

A new direction is emerging in the field of spintronics [1–4], where one wants to inject spin currents, transfer and manipulate the spin information, and detect the resulting spin polarization in nonmagnetic metals and semiconductors. A first and successful attempt to electrically inject and detect spins in metals dates back to 1985 when Johnson and Silsbee successfully demonstrated spin accumulation in a single crystal aluminium bar up to temperatures of 77 K. [5,6] In their pioneering experiments they were able to observe spin precession of the induced non-equilibrium magnetization. However, the measured signals were extremely small (in the pV range), due to the relatively large sample dimensions as compared to contemporary technology.

In this letter we report spin precession in a diffusive Al strip at RT. The use of tunnel barriers at the ferromagnetic metal-nonmagnetic metal (F/I/N) interface and the reduced sample dimensions by 3 orders of magnitude, has increased the output signal (V/I) of our device by 6 orders of magnitude as compared to ref. [5]. We find a spin relation length $\lambda_{sf} = 500$ nm in the Al strip at RT, which is within a factor of 2 of the maximal obtainable spin relaxation length at RT, being limited by the inelastic phonon scattering processes. At lower temperatures larger spin relaxation lengths can be obtained by reducing the impurity scattering rate, as was previously reported. [4–6]

The samples are fabricated by means of a suspended shadow mask evaporation process [7,8] and using electron beam lithography for patterning. The shadow mask is made from a tri-layer consisting of a $1.2 \mu\text{m}$ PMMA-MA base layer (Allresist GMBH ARP 680.10 in methoxy-ethanol), a 40 nm thick germanium (Ge) layer and on top a 200 nm thick PMMA layer (Allresist GMBH ARP 671.04 in chlorobenzene). The base and top resist layers have different sensitivities for e-beam radiation, which enables a selective exposure by varying the induced charge dose ($400 \mu\text{C}/\text{cm}^2$: both layers, $100 \mu\text{C}/\text{cm}^2$: base layer) by the e-beam.

In the first development step the top layer is developed, followed by an anisotropic CF_4 dry etching to remove the

exposed germanium layer. In a third (wet) development step the PMMA-MA base layer underneath the Ge layer is developed resulting in a suspended shadow mask, see the inset of Fig. 1a.

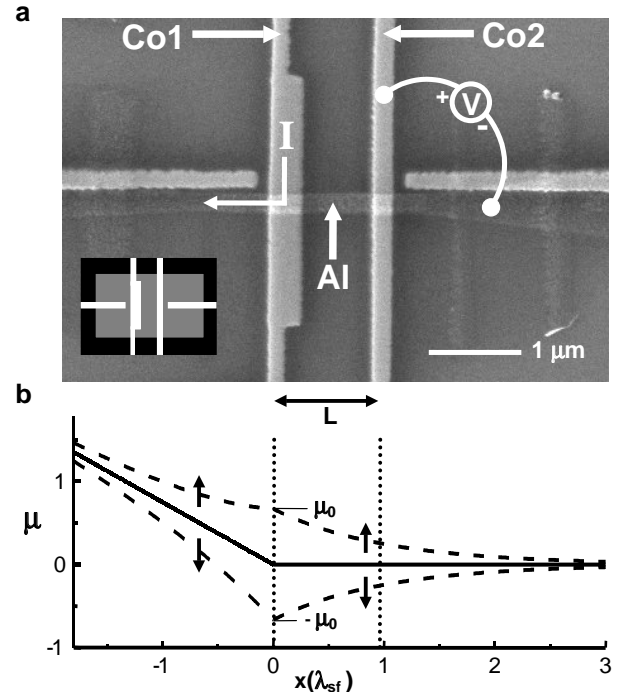


FIG. 1. (a) SEM-picture of the spin valve device. The current I is injected from Co1 into the Al strip (left side) and the voltage V is measured between Co2 and the Al strip (right side). Inset: center of the tri-layer shadow mask (see text). Black: PMMA-MA/Ge bilayer. White: SiO_2 substrate. Grey: suspended Ge layer. (b) The spatial dependence of the spin-up and spin-down electrochemical potentials (dashed) in the Al strip. The solid lines indicate the electrochemical potential (voltage) of the electrons in the absence of spin injection.

In a last step, the top resist layer is etched away by using an oxygen plasma. After completion of the mask, a two step shadow evaporation procedure is used to make

the sample. First we deposit an Al layer from the left and right side (see inset Fig. 1a) under an angle of 25° with the substrate surface at a pressure of 10^{-6} mbar, thus forming a continuous Al strip underneath the suspended Ge mask with a thickness of 50 nm.

Next, without breaking the vacuum, an Al_2O_3 oxide layer is formed at the Al surface due to a 10 minutes O_2 exposure at 5×10^{-3} mbar. In a third step, after the vacuum is recovered, a 50 nm thick Co film is deposited from below (see inset Fig. 1a) under an angle of 85° with the substrate surface. In Fig. 1a a SEM picture is shown of a sample with a Co electrode spacing of $L = 1100$ nm. The conductivity of the Al and Co strips were determined to be $\sigma_{\text{Al}} = 1.3 \cdot 10^7 \Omega^{-1}\text{m}^{-1}$ and $\sigma_{\text{Co}} = 4.1 \cdot 10^6 \Omega^{-1}\text{m}^{-1}$, whereas the resistance of the Al/ Al_2O_3 /Co tunnel barriers were determined to be 800Ω for the Co1 electrode and 2000Ω for the Co2 electrode at RT.

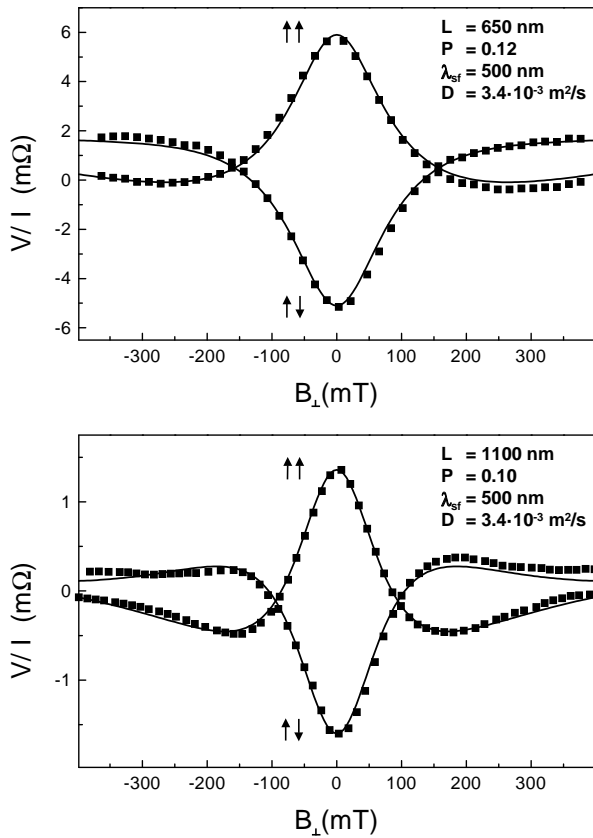


FIG. 2. Modulation of the output signal (V/I) due to spin precession as a function of a perpendicular magnetic field B_\perp , for $L=650$ nm and $L=1100$ nm. The solid squares represent data taken at RT, whereas the solid lines represent the best fits based on eq. 4. We note that the fits incorporate the effect of a slight tilting of the magnetization direction of the Co electrodes out of the substrate plane, see Ref. 4.

In our experiment we inject a spin polarized current ($I = 100 \mu\text{A}$) from the Co1 electrode via a tunnel barrier into the Al strip. The spin polarization P of the current is determined by the ratio of the different spin-up and spin-

down tunnel barrier resistances R_\uparrow^{TB} and R_\downarrow^{TB} , which in first order can be written as $P = (N_\uparrow - N_\downarrow)/(N_\uparrow + N_\downarrow)$. [9] Here $N_\uparrow(N_\downarrow)$ is the spin-up (spin-down) density of states at the Fermi level of the electrons in the Co electrodes. The unequal spin-up and down currents cause the electrochemical potentials (densities) $\mu_\uparrow, \mu_\downarrow$ of the spin-up and spin down electrons in the Al strip to become unequal, see Fig. 1b. The spatial dependence of $\mu_\uparrow, \mu_\downarrow$ can be calculated by solving the 1-dimensional spin coupled diffusion equations in the Al strip. [10,11] For $x \geq 0$, we obtain:

$$\mu(x)_\uparrow = \mu_0 \exp\left(\frac{-x}{\lambda_{sf}}\right) \quad \text{and} \quad \mu(x)_\downarrow = -\mu_0 \exp\left(\frac{-x}{\lambda_{sf}}\right), \quad (1)$$

where $\mu_0 = \frac{eI\lambda_{sf}P}{2A\sigma_N}$ and $\lambda_{sf} = \sqrt{D\tau_{sf}}$, D , τ_{sf} , σ_N and A are the spin relaxation length, diffusion constant, spin relaxation time, conductivity and cross sectional area of the Al strip.

At a distance L from the Co1 electrode the induced spin accumulation ($\mu_\uparrow - \mu_\downarrow$) in the Al strip can be detected by a second Co2 electrode via a tunnel barrier. The detected potential is a weighted average of μ_\uparrow and μ_\downarrow due to the spin dependent tunnel barrier resistances:

$$\mu_d = \frac{\pm P(\mu_\uparrow - \mu_\downarrow)}{2} + \frac{(\mu_\uparrow + \mu_\downarrow)}{2}, \quad (2)$$

where the $+$ ($-$) sign corresponds with a parallel (anti-parallel) magnetization configuration the Co electrodes. Using eqs. 1 and 2 we can calculate the magnitude of the output signal (V/I) of the Co2 electrode relative to the Al voltage probe at distance L from Co1:

$$\frac{V}{I} = \frac{\mu_d - \mu_N}{eI} = \pm \frac{P^2\lambda_{sf}}{2A\sigma_N} \exp\left(\frac{-L}{\lambda_{sf}}\right), \quad (3)$$

where $\mu_N = (\mu_\uparrow + \mu_\downarrow)/2$ is the measured potential of the Al voltage probe. Equation 3 shows that in absence of a magnetic field the output signal decays exponentially as a function of L . [4]

However, in the experiment the injected electron spins in the Al strip are exposed to a magnetic field B_\perp , directed perpendicular to the substrate plane and the initial direction of the injected spins being parallel to the long axes of Co electrodes. Because B_\perp alters the spin direction of the injected spins by an angle $\phi = \omega_L t$ and the Co2 electrode detects their projection onto its own magnetization direction (0 or π), the spin accumulation signal will be modulated. Here $\omega_L = g\mu_B B_\perp/\hbar$ is the Larmor frequency, g is the g-factor of the electron (2 for Al), μ_B is the Bohr magneton, \hbar is Planck's constant divided by 2π and t is the diffusion time between Co1 and Co2. The observed modulation of the output signal as a function of B_\perp at RT is shown in Fig. 2.

For a parallel $\uparrow\uparrow$ (anti-parallel $\uparrow\downarrow$) configuration we observe an initial positive (negative) signal, which drops in amplitude as B_\perp is increased from zero field. This is called the Hanle effect in Refs. [5,6]. The parallel

and anti-parallel curves cross each other where the average angle of precession is about 90 degrees and the output signal is close to zero. As B_{\perp} is increased beyond this field, we observe that the output signal changes sign and reaches a minimum (maximum) when the average angle of precession is about 180 degrees, thereby effectively converting the injected spin-up population into a spin-down and vice versa. We have fitted the data with eq. 4 and using $\lambda_{sf} = 500$ nm, $\sigma_N = e^2 N D$ and $N = 2.4 \cdot 10^{28}$ states/eV/m³ [12] we find the spin relaxation time $\tau_{sf} = 65$ ps in the Al strip at RT to be in good agreement with theory. [13] We note that half of the momentum scattering processes at RT is due to phonon scattering, which implies that the spin relaxation length can be maximally improved by a factor of 2. A detailed discussion about spin relaxation times is given in [14].

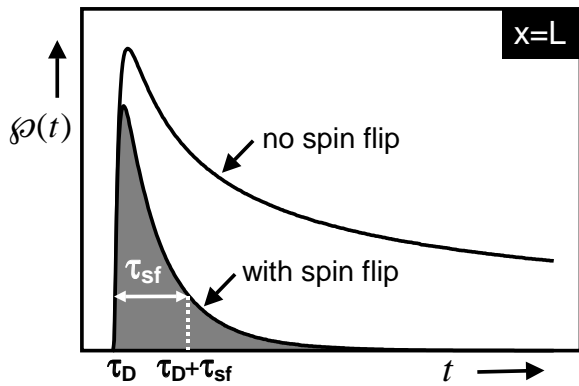


FIG. 3. Probability per unit volume that, once an electron is injected, will be present at $x = L$ without spin flip ($\phi(t)$) and with spin flip ($\phi(t) \cdot \exp(-t/\tau_{sf})$), as a function of the diffusion time t .

Figure 2 shows the amplitude of the oscillating output signal decays with increasing B_{\perp} , caused by the diffusive nature of the Al strip. In an (infinite) diffusive 1D conductor the diffusion time t from Co1 to Co2 has a broad distribution $\phi(t) = \sqrt{1/4\pi Dt} \cdot \exp(-L^2/4Dt)$, where $\phi(t)$ is proportional to the number of electrons per unit volume that, once injected at the Co1 electrode ($x=0$), will be present at the Co2 electrode ($x = L$) after a diffusion time t . Therefore the output signal (V/I) is a summation of all contributions of the electron spins over all diffusion times t :

$$\frac{V(B_{\perp})}{I} = \pm \frac{P^2}{e^2 N(E_F) A} \int_0^{\infty} \phi(t) \cos(\omega_L t) \exp\left(\frac{-t}{\tau_{sf}}\right) dt. \quad (4)$$

In Fig. 3 $\phi(t)$ is plotted as a function of t , showing that the integral of $\int_0^{\infty} \phi(t) dt$ is diverging. So even when τ_{sf} is infinite the broadening of diffusion times will destroy the spin coherence of the electrons present at Co2 and hence will lead to a decay of the output signal. However, a sign reversal of the output signal is still observed because only the electrons present at Co2 carrying their

spin information are relevant. The exponential factor in the integral of eq. 4, describing the effect of the spin flip scattering, will cut off the diffusive broadening of $\phi(t)$ and create a window of diffusion times from τ_D to $\tau_D + \tau_{sf}$, see Fig. 3. Here $\tau_D = L^2/2D$ is the diffusion time corresponding to the peak of $\phi(t)$ in absence of spin flip scattering. The condition to observe more than a half period of modulation imposes $\phi_{ave} = \omega_L \tau_D \geq \pi$, whereas a limitation on the diffuse broadening imposes the condition $\Delta\phi = \omega_L \tau_{sf} \leq \pi$. Using $\tau_D = L^2/2D$ we find with this simplified picture that the requirement in order to observe at least half a period of oscillation is approximately given by: $L \geq \sqrt{2} \lambda_{sf}$.

Using the program Mathematica we can solve the integral $Int(B_{\perp}) = \int_0^{\infty} \phi(t) \cos(\omega_L t) \exp\left(\frac{-t}{\tau_{sf}}\right) dt$ and we find:

$$Int(B_{\perp}) = Re\left(\frac{1}{2\sqrt{D}} \frac{\exp\left[-L\sqrt{\frac{1}{D\tau_{sf}} - i\frac{\omega_L}{D}}\right]}{\sqrt{\frac{1}{\tau_{sf}} - i\omega_L}}\right). \quad (5)$$

Equation 5 shows that in the absence of precession ($B_{\perp} = 0$) the exponential decay of eq. 3 is recovered. It can be shown by using standard goniometric relations that eq. 5 is identical to the solution describing spin precession obtained by solving the Bloch equations with a diffusion term. [6] In particular we find $Int(B_{\perp}) = \frac{1}{2} \frac{\sqrt{\tau_{sf}}}{2D} F_1\{b, l\}$, where $F_1\{b, l\}$ is derived in Ref. [6], $b \equiv \omega_L \tau_{sf}$ is the reduced magnetic field parameter and $l \equiv \sqrt{\frac{L^2}{2D\tau_{sf}}}$ is the reduced injector-detector separation parameter.

To conclude, we have demonstrated spin precession in an Al strip at RT. As a final note we believe that our obtained value $P \approx 10\%$ [15] is too low and we anticipate that the output signal of our device can be improved by more than an order of magnitude by improving the material properties of the Co material. [16] The authors wish to thank the Stichting Fundamenteel Onderzoek der Materie (FOM) and NEDO (project 'Nano-scale control of magnetoelectronics for device applications') for financial support.

-
- [1] Semiconductor spintronics and Quantum Computation, Editors: D.D. Awschalom, D.Loss, N. Samarth, Springer Nanoscience and technology series, (2002)
 - [2] S. A. Wolf *et al.*, Science **294**, 1488 (2001).
 - [3] F.J. Jedema, A. T. Filip, and B.J. van Wees, Nature **410**, 345 (2001).
 - [4] F.J. Jedema, H.B. Heersche, A.T. Filip, J.J.A. Baselmans, B.J. van Wees, Nature **416**, 713 (2002)
 - [5] M. Johnson and R. H. Silsbee, Phys. Rev. Lett. **55**, 1790 (1985)

- [6] M. Johnson and R.H. Silsbee, Phys. Rev. B **37**, 5326 (1988)
- [7] G. J. Dolan, Appl. Phys. Lett., **31**, 337(1977).
- [8] L.D. Jackel, R.E. Howard, E.L.Hu, D.M. Tennant and P. Grabbe, Appl. Phys. Lett. **39**, 268 (1981)
- [9] M. Julliere, Phys. Rev. Lett. **54**, 224-227 (1975).
- [10] P.C. van Son, H. van Kempen, and P. Wyder, Phys. Rev. Lett. **58**, 2271 (1987)
- [11] T. Valet and A. Fert, Phys. Rev. B **48**, 7099 (1993)
- [12] D. A. Papaconstantopoulos, - Handbook of the band structure of elemental solids, New York; London : Plenum, 1986.
- [13] J. Fabian, S. Das Sarma, Phys. Rev. Lett. **83**, 1211 (1999).
- [14] F.J. Jedema, M. Nijboer, B.J. van Wees, submitted to Phys. Rev. B
- [15] R. Meservey and P. M. Tedrow, Physics Reports **238**, 173 (1994).
- [16] W.F. Egelhoff *et al.*, J.Appl.Phys. **79**, 5277 (1996)